
MUTE: Data-Similarity Driven Multi-hot Target Encoding for Neural Network Design

Mayoore S. Jaiswal¹ Bumsoo Kang^{2*} Jinho Lee^{3 †} Minsik Cho¹

¹IBM, Austin, TX, USA ²KAIST, Daejeon, South Korea ³Yonsei University, Seoul, South Korea
mayoore.s.jaiswal@ibm.com, minsikcho@us.ibm.com

Abstract

Target encoding is an effective technique to deliver better performance for conventional machine learning methods, and recently, for deep neural networks as well. However, the existing target encoding approaches require significant increase in the learning capacity, thus demand higher computation power and more training data. In this paper, we present a novel and efficient target encoding scheme, MUTE to improve both generalizability and robustness of a target model by understanding the inter-class characteristics of a target dataset. By extracting the confusion level between the target classes in a dataset, MUTE strategically optimizes the Hamming distances among target encoding. Such optimized target encoding offers higher classification strength for neural network models with negligible computation overhead and without increasing the model size. When MUTE is applied to the popular image classification networks and datasets, our experimental results show that MUTE offers better generalization and defense against the noises and adversarial attacks over the existing solutions.

1 Introduction

Scalable artificial intelligent systems require a methodology for efficient neural network design that can generalize well, learn semantics of the training dataset, and resist adversarial attacks. However, existing methods have been shown to learn dataset bias [30, 29, 23], and failed to deliver sufficient generalization capability. Poor generalization makes models unpredictable, causes potential ethical issues, and mis-guides neural network design [36, 10]. To tackle the generalization problems, target encoding has been studied for both conventional machine learning and deep neural network architectures and proven to be highly effective [2, 9, 15, 5]. Yet, many prior works in target encoding require a long encoding sequence (which increases the model size) and fail to tailor the encoding for a given task or dataset. Furthermore, they do not investigate the effects of different target encodings against noisy data and adversarial attacks.

In this work, we propose MUTE, a systematic approach to make deep learning models generalize better by optimizing the target encoding [2, 9, 15, 5]. Unlike the conventional one-hot method where the Hamming distance between labels is fixed at 2, MUTE generates a multi-hot encoding by exploiting the expression power of a given output encoding length. MUTE strategically extracts the *similarity* between pairs of classes from a dataset, and leverages that information to obtain a multi-hot encoding such that semantically closer classes are forced to be further apart in the label space in terms of the Hamming distance. MUTE ensures that Stochastic Gradient Decent (SGD) algorithm extracts distinctive features between two easy-to-confuse classes, which in turn reduces the chance of mis-prediction under noisy and noiseless conditions. Figure 1 illustrates the high-level idea in MUTE, that is it increases the distance between classes in feature space. In order to find such high-quality

*Work done during internship at IBM

† Work done while at IBM

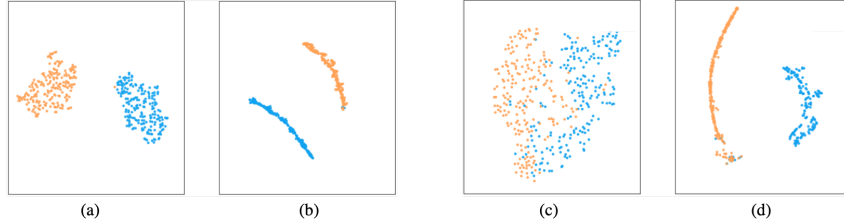


Figure 1: TSNE [24] visualizations of a ConvNet (refer Section 4.2 for architecture) with one-hot encoding trained on MNIST (a, c) and a ConvNet with MUTE trained on MNIST (b, d). Classes well-separated in features space in models trained with one-hot encodings (a), remain well separated in models trained with MUTE (b). However, class not-well-separated in features space in models trained with one-hot encodings (c), are well-separated in feature space when trained with MUTE.

encoding in MUTE, we formulate the encoding generation as a subgraph isomorphism problem [32] and develop efficient heuristics to solve the combinatorics.

We evaluate MUTE by training multiple convolutional neural network (CNN) architectures with benchmark datasets such as MNIST [22], CIFAR-10 [18] and ICON-50 [13], and testing on a validation set which consists of original, noisy (i.e., negative of the original images, Gaussian blurred images, images with salt-and-pepper noise) and adversarial images similar to real-world conditions. Our results show that the models built by MUTE did not lose any accuracy against the original clean images, yet delivered better test accuracies against noisy images than the traditional one-hot encoding and prior work, especially when the learning capacity of a model is limited. Our contributions in MUTE include the following: **a)** novel target encoding scheme based on weighted Hamming distance, **b)** effective heuristics for subgraph isomorphism in the target encoding context, and **c)** comprehensive study on the effects of our target encoding scheme on both noisy and adversarial images.

2 Related Work

In this section, we will briefly review various encoding techniques used in deep learning. Please refer to the supplementary material (SM) for an extended review.

Multi-class Single-label: This is the traditional one-hot (1-of-N) encoding scheme that is popularly used in deep learning. One-hot encoding simply represents the target labels numerically without any semantic meaning and is prone to noisy inputs or adversarial attacks [13, 28, 25, 11].

Multi-class Multi-label: This is the superposition of multiple one-hot encodings for the case where a sample belongs to multiple semantic classes [15, 5]. This contrasts with multi-hot encoding (i.e. MUTE) where a sample belongs to only one class, but represented in multiple bits.

Label Embedding: This is a technique to embed target labels with meta information like attributes [2] or hierarchies [31] to capture various structures of the output space at the cost of additional labelling and expert knowledge [9, 15]. In some cases, the embedding is jointly learned from input and output data [3, 33].

Target Encoding: These are methods that explore alternatives to one-hot encoding [17, 7, 21, 20, 6, 27], similar to MUTE. Yet, the key innovations in MUTE over them are as follows: **a)** MUTE has the same encoding length as one-hot unlike [17], and could be used as a drop-in-replacement of any existing one-hot encoding, **b)** MUTE strategically optimizes the encoding w.r.t. the given class distribution. Extended review on Target Encoding is in SM.

3 Data-Similarity Driven Multi-hot Target Encoding

We propose a new target encoding system, MUTE, where multiple output bits are activated. For an N -class classification problem with MUTE, the output layer has N -bits, out of which K bits are 1s as chosen, where $K > 1$. Each output bit has a bounded non-linear activation function and trained such that the binary cross entropy loss between the prediction and target label is minimized.

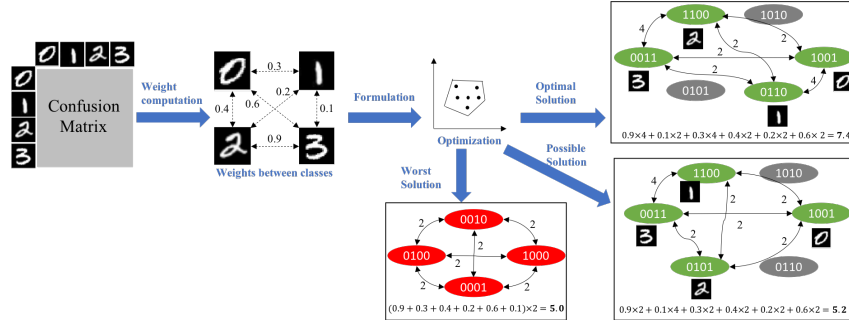


Figure 2: Flow chart of multi-hot encoding generation in MUTE.

The core idea in MUTE is to evaluate the similarity between a given set of classes, then leverage that information to build robust neural networks. To that end, first, the similarity between classes in a given dataset is measured. These similarity weights are used to generate a set of target codes such that the Hamming distances among all classes are maximized and a pair of similar classes are assigned codes with larger Hamming distance based on the extent of similarity. This increases the distance between classes in the feature space as illustrated in Figure 1, thereby reducing the probability of mis-prediction, increasing the generalization of the classifier, and forcing a model to learn the semantics rather than spatial correlation among pixels. Any chosen neural network could be trained and tested with the generated target encoding without increasing the number of parameters. Overall flow of the encoding generation is in Figure 2, which will be discussed in the following sections.

3.1 Generating Weights For Target Codes

When a deep neural network is trained with back-propagation, it is being optimized to learn features that distinguish classes. When it is able to learn distinct features, these classes are well separated in feature space and have a low probability of mis-prediction (Figure 1(a),(b) and (d)). However, when a network is not able to learn distinguishable features, these classes are not well separated, which may result in poor accuracy (Figure 1(c)). The hypothesis is to identify such visually similar classes and assign target codes that have high Hamming distance between them. By training with such target codes, the network is optimized to learn features to separate similar classes. Having clear decision boundaries between classes help to reduce classification error and better performance with noisy and adversarial images.

The objective of this step is to quantitatively identify similar classes and assign weights to the level of similarity. A confusion matrix (CM) is a known method to represent inter-class similarities. CM is essentially a $N \times N$ matrix for a N -class dataset with the elements being the confusion metric between a pair of classes as shown in Figure 2 (top-left). CM can be obtained by inferencing using a validation set on an already trained target model. We use the method proposed in [4] to generate CM where the confusion-level between classes of a dataset can be determined by reconstructing data for each class using an autoencoder trained using class C_i and determining the reconstruction error for every other class C_j in the dataset. Once CM is obtained for a given dataset, MUTE can convert the confusion matrix into weights (to be used in Section 3.2) in the following method: the weights are obtained by subtracting the diagonal of CM (self-error values) from CM , finding the minimum error of the upper and lower triangles of CM , thresholding larger errors to eliminate dissimilar classes, and scaling the non-zero values of CM .

3.2 Generating Target Codes

With weights obtained from Section 3.1, the next step in MUTE is to generate a set of multi-bit target encoding. Our goal is two-fold: **a)** to generate encoding that maximize Hamming distances among all encoding and **b)** to assign a pair of encoding that has larger Hamming distance to a pair of more similar classes. In this light, we generate encodings that maximize the total minimum Hamming distance and the Hamming distances between classes based on inter-class similarities.

Inter-class similarities are taken into account in our objective function as weights of Hamming distances over pairs of classes. We put the total minimum Hamming distance and weighted Hamming distances together in our objective function as in Equation 1.

$$W_{min}H_{min} + \sum_{i=0}^{N-1} \sum_{j=i+1}^N W_{ij}H_{ij} \quad (1)$$

where W_{min} denotes the weight of the minimum Hamming distance H_{min} , N denotes the total number of classes, W_{ij} and H_{ij} denote inter-class similarity and the Hamming distance between class i and class j , respectively. N and W_{ij} are given constants (i.e., W_{ij} is computed as in Section 3.1). W_{min} should be larger than W_{ij} because maximizing H_{min} drives the overall model performance. We set W_{min} as the number of pairs of classes, $N(N-1)/2$, in our experiments. In one-hot encoding, H_{min} is fixed at 2, while H_{min} is maximized in MUTE.

Figure 2 shows an example of possible outcomes from the optimization step. With one-hot encoding (bottom-center), there exists one trivial solution and the weighted sum of the Hamming distances is the lowest among the solutions illustrated. Figure 2 also shows the difference between the optimal and a possible solution in terms of the Hamming distance and the generated encoding: the optimal solution picks a set of encoding and assigns them to the four classes such that more similar classes (i.e., 2 vs. 3 with weight 0.9) are assigned to two codes with the larger Hamming distance.

Optimization in Figure 2 can be formulated as an Integer Linear Programming (ILP) due to the discrete nature of the encoding itself, and solved by a commercial package. However, it requires a large amount of computation time to find an optimal solution because it explores solution space in an exhaustive branch-and-bound manner. Yet, one useful observation about this combinatorics is that the distribution of Hamming distance values are very discrete and narrow, and has high-density only on a few integer values. Therefore, we expect that there should be a number of possible solutions that have the same objective values. In other words, this maximization problem has a wide and sparse solution space, allowing us to develop an efficient heuristic, **Narrow-convergence Approach** for MUTE, which is inspired from [8] and finds a solution to Equation 1 significantly faster than ILP optimizations in the following steps:

- **S0:** Equation (1) with $W_{ij} = 1$ is optimized as ILP for a given number of classes and bits for a short amount of time until it sufficiently narrows down the solution space. The time limit depends on the number of classes, N , and the number of bits, K .
- **S1:** Capture the intermediate result from Step **S0** to form a set of initial encodings, \mathcal{E} .
- **S2:** Pick one class randomly without replacement from \mathcal{E} .
- **S3:** Choose a small set of alternative encodings for the chosen class, and put them into the candidate pool, \mathcal{P} .
- **S4:** Pick the encoding that maximizes Equation (1) from \mathcal{P} , and assign the encoding to the chosen class. **S2-S4** is repeated until every class is updated.
- **S5:** Go back to Step **S2** until no further improvement in the objective function is found (otherwise exit).

The main difference between ILP optimization and narrow-convergence approach is the strategy for finding solutions. ILP takes a breadth-first search strategy to find an optimal solution, whereas our approach takes a depth-first search strategy. A formal description of Narrow-convergence Approach is available in the supplementary material.

3.3 Training Method

The MUTE could be used with any CNN model with no changes to the architecture. The traditional softmax classification layer is replaced with a sigmoid layer. The CNN is trained by back-propagating the binary cross entropy loss at each bit. CNN is optimized by SGD with momentum. An overview of training a CNN with MUTE is given in Figure 3a. In this method, the number of neurons in the CNN and the computational complexity is the same as using one-hot target encoding.

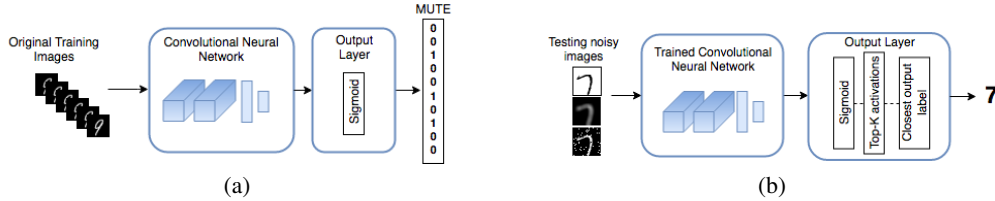


Figure 3: Overview of the (a) training and (b) inferring methods

3.4 Inferencing Method

As shown in Figure 3b, an input image is forward propagated through the trained model. The output of the sigmoid layer is thresholded by setting all but the $top - K$ activated bits to 0, where K is the number of bits used in the MUTE. Then, the Euclidean distance between the thresholded output and each of MUTE encodings are computed. The label corresponding to the closest MUTE code is the classification result. In the one-hot case, the model has to activate only 1 bit to deliver a classification. In the proposed method, the model has to activate K output bits to deliver a classification. Even if one or two bits flip due to noise, it may not change the nearest label. Hence, error correcting code MUTE is able to deliver the correct prediction despite noise. Computing Euclidean distance between the set of target encoding may have a potential impact on inference latency. The latency could be minimized by optimizing the Euclidean distance computation using a fast XOR method.

4 Results & Discussion

4.1 Generation of MUTE

We compared our Narrow-convergence Approach with ILP optimization using CPLEX [1] in terms of the solution quality and computation time (Table 1). We broke-down ILP optimization into two approaches: optimization with weights, and optimization without weights followed by shuffling with weights. The experiment was to generate 10bits/4-hot target encodings for 10 classes. Our experiment environment includes 56 CPU cores with 120GB RAM memory. CPLEX ran with parallel threads utilizing 32 cores in the experiment.

	Optimization approach	Objective value	Min. Hamming distance	Computation time
10-bit 4-hot	Narrow-convergence	450.21	4	90 sec
	CPLEX (w/ weights)	450.31	4	> 11 hrs
	CPLEX (w/o weights)	447.75	4	> 50 hrs

Table 1: Ours reduced run-time by more than 99.75% compared to conventional ILP.

For the 4-hot/10bits case with weights derived from MNIST dataset, narrow-convergence approach reduced the time cost by more than 99.75%, while it performs as good as ILP optimization. ILP with weighted objective function takes more than 11 hours to reach an objective value of 450.31. We were not able to run more than 11 hours due to memory limitations. Solving unweighted objective function for 50 hours followed by shuffling with weights reaches an objective value of 447.75.

4.2 Performance of MUTE

Datasets. We used the MNIST [22], CIFAR-10 [18] and ICON-50 [13] datasets for experiments. MNIST is a dataset of handwritten digits in black and white containing 60,000 training images and 10,000 testing images. CIFAR-10 is a dataset of 32×32 color images belonging to 10 classes representing airplanes, cars, birds, cats, deer, dogs, frogs, horses, ships, and trucks. It has 50,000 training and 10,000 testing images equally distributed among its classes. ICON-50 is a set of 10,000 color icons of size 32×32 belonging to 50 classes such as airplane, ball, drink, feline, etc., and collected from various companies such as, Apple, Microsoft, Google, Facebook, etc. The icons from different companies exhibit different styles and versions. This is a challenging dataset because there is a class imbalance between icons collected from various companies (in other words different styles).

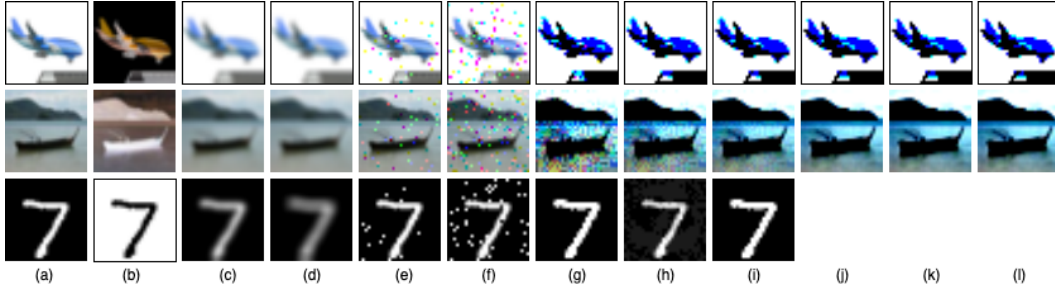


Figure 4: Images from the various test sets. The images in the first row is from the ICON-50 [13] dataset, second row is from the CIFAR-10 [18] dataset and the third row is from the MNIST [22] dataset. (a) Original images. (b) Negative [14] of the original images. (b - d) Original images blurred with Gaussian kernels of $\sigma = 1$ and $\sigma = 2$ respectively. (e - f) Salt & pepper noise added to the original images at 2% and 5% respectively. (g - l) Adversarial images with FGSM [11] noise with $\epsilon = 0.2, 0.1, 0.05, 0.01, 0.005$ and 0.001 respectively.

CNN Architectures. We utilized a wide range of CNN architectures in our experiments. MNIST dataset was trained and tested with two CNNs: LeNet [22] and ConvNet. ConvNet has 2 convolutional layers with 5×5 kernel size, followed by a fully connected layer with 50 neurons and a final sigmoid layer. CIFAR-10 and ICON-50 datasets are trained and tested with AlexNet [19], DenseNet [16], ResNet [12], and ResNeXt [34] architectures. DenseNet has depth of 40 and growth rate of 24. ResNet has depth of 20. ResNeXt has depth of 29 and cardinality of 8.

Experiments. We used the standard train/test split for MNIST and CIFAR-10 datasets. For ICON-50, 80% of images in each class were randomly assigned to the training set and rest were allocated to the test set. Various CNN architectures were trained with original images in the training dataset for 200 epochs. The trained models were tested with original images in the test set. Additionally, to evaluate the robustness of the trained models, we created and tested noisy versions of the original test sets as shown in Figure 4. Negative images [14] have the same spatial structure as the original images but are in a diagonally opposite color space. These images are useful to evaluate if the trained models have learned the semantic structure of the dataset or merely memorized the spatial pixel correlations in the training images. Typical noisy images such as Gaussian blurred images with $\sigma = 1$ and 2 and Salt & Pepper noise at 2% and 5% were created. To test robustness against adversarial attacks, we created adversarial images with Fast Gradient Sign Method (FGSM) [11] with $\epsilon = 0.05, 0.1$ and 0.2 . This creates a comprehensive test set that evaluates models for their generalization and robustness capability.

In our experiments, we compared against the conventional one-hot encoding and Hadamard target encoding methods. In addition to comparing with Hadamard encoding results in [35], we substituted the proposed MUTE with Hadamard encodings [35] and trained and tested on the chosen datasets. Hadamard results are shown as H-63, H-127 and H-255 in the Figures 5 and 6. We also conducted experiments with weighted and unweighted MUTE for different number of hot bits. The results of our experiments are shown in Figures 5, 6, 7, 8 and Table 2.

We trained models with various target encodings with the same set of hyper-parameters to eliminate the impact of hyper-parameter choice on the model performance. We did not augment MNIST, however augmented CIFAR-10 and ICON-50 data using randomized affine transformations, color jitter and cropping in random order. The augmentation parameters were chosen by trial and error. The batch size was 128. CNNs were optimized using SGD with 0.9 momentum, 0.0001 weight decay, and 0.1 initial learning rate. All experiments were conducted on an Intel(R) machine with Xeon(R) CPU E5-2680 v4 at 2.40 GHz frequency. It has 504 GB RAM and 56 CPU cores. The machine has 4 Tesla P100-PCIE GPUs. Models were trained using only 1 GPU at a time. Code was written using PyTorch V1 [26] implementation.

Figure 5 shows the test accuracy of LeNet and ConvNet architectures with different target encodings trained on original images in the MNIST training dataset and tested on original, noisy and adversarial versions of the MNIST test dataset. The barplots illustrate the central tendency for different test datasets and uncertainty (error bars) for test images impacted by varying amounts of Gaussian blur,

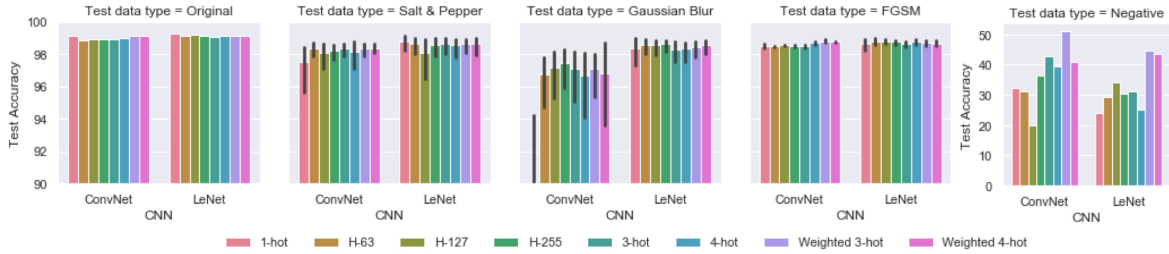


Figure 5: MUTE with LeNet and ConvNet architectures trained on MNIST data improves the one-hot average test accuracy by 2.8% and 7.1% respectively. Whereas Hadamard target encoding improves one-hot performance only by 1.7% and 3.5%.

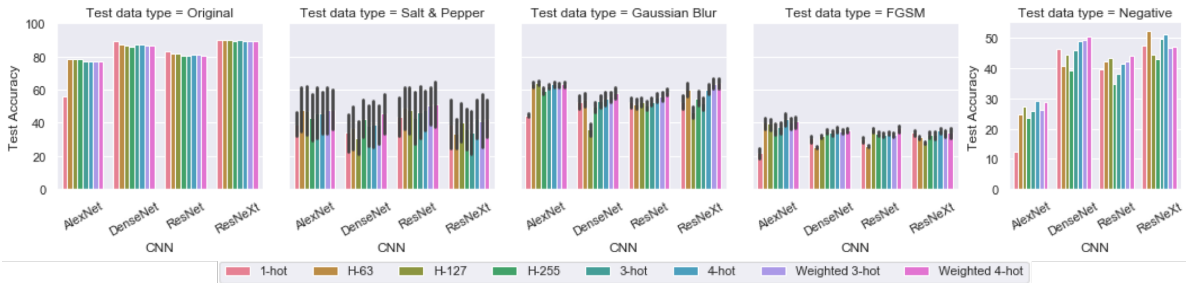


Figure 6: MUTE encoding with AlexNet, DenseNet, ResNet and ResNeXt architectures trained on CIFAR-10 data improves the one-hot average test accuracy by 41.5% , 4.2%, 3.6% and 3.8% respectively. Whereas Hadamard target encoding improves one-hot performance only when used with AlexNet and ResNet architecture. When used with DenseNet and ResNeXt, the average test accuracy is worse than using one-hot encoding.

Salt & Pepper noise and FGSM. The proposed MUTE method has better average test performance than one-hot encoding or Hadamard target encoding (H-63, H-127, and H-255). The best test accuracy on original images reported by [35] using Hadamard Codes on MNIST is 85.47% using direct classification with H-255. The authors [35] use a CNN architecture with 3 convolutional layers, 1 locally connected layer and 2 fully-connected layers. The proposed MUTE method improves this result by 13.61 percentage points on average.

CNN architectures with various MUTE were trained on original images in the CIFAR-10 training dataset and tested on original and noisy versions of the CIFAR-10 test dataset as shown in Figure 6. The proposed MUTE method with AlexNet, DenseNet, ResNet and ResNeXt architectures improved average test accuracy over one-hot encoding. However, choice of architecture seems to be important when using Hadamard encodings, as performance dropped when using DenseNet and ResNeXt architectures. MUTE is particularly useful when a less robust architecture such as AlexNet [13] is used.

We trained AlexNet, DenseNet, ResNet, and ResNeXt architectures on an ICON-50 training set that contained images from all 50 classes and tested on original and noisy images in the test set (Figure 7). MUTE increased one-hot encoding performance 0.3% to 42.29% with AlexNet, the least robust CNN [13], benefiting the most from MUTE. In another experiment using Icon-50 dataset, we

CNN Arch.	Target Encoding				
	1-hot	15-hot	20-hot	Weighted 15-hot	Weighted 20-hot
AlexNet	21.85	33.78	34.45	32.72	32.83
DenseNet	31.02	34.07	33.72	31.77	34.95
ResNet	29.87	32.31	31.56	32.21	33.31
ResNeXt	34.68	34.86	34.66	34.51	34.76

Table 2: Average test accuracy on noisy data of the ICON-50 sub-type robustness experiment in [13].

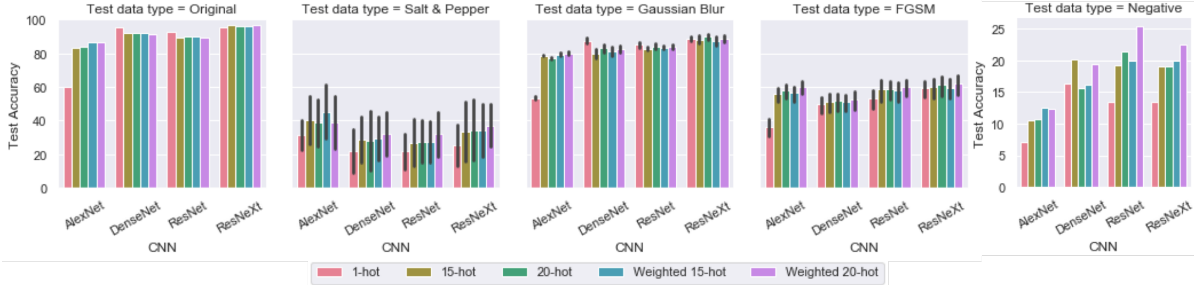


Figure 7: AlexNet, DenseNet, ResNet, and ResNeXt architectures trained with various MUTE on ICON-50 data and tested with the original and noisy testsets improved average test accuracy over one-hot by 42.29%, 0.37%, 4.70%, and 8.12% respectively.

trained the CNN architectures on all original images belonging to the sub-type robustness experiment in [13]. Then tested on the noisy versions (negative, Gaussian blurred, and Salt & Pepper noise) of the held-out sub-types. Table 2 lists the average test accuracy on the noisy test sets. MUTE consistently obtains higher average test accuracy for any number of hot bits or weighted configuration. We used the TSNE [24] algorithm to visualize ConvNet and AlexNet models trained with one-hot and MUTE on MNIST and CIFAR-10 datasets, respectively. Figure 8 shows that models trained with one-hot encodings fail to learn distinguishable features that give rise to good decision boundaries. Thus, noisy data is easily mis-predicted. On the other-hand, condensed features learned by MUTE enable clear decision boundaries even when faced with noisy data.

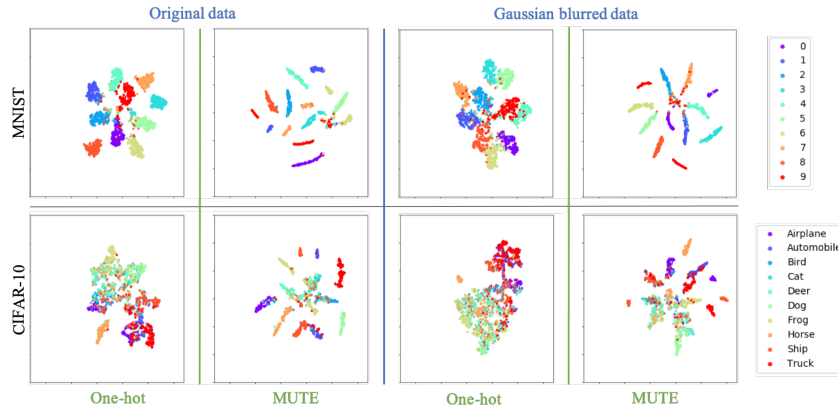


Figure 8: Features learned with MUTE are well-separated and condensed in multi-dimensional space such that model maintains separation even when tested with noisy data. In comparison, features learned by one-hot encodings lack isolation in feature space.

5 Conclusion

We propose a novel target encoding methodology that is cognizant of inter-class similarities to train neural networks. We proposed Narrow-convergence Approach, a time-effective method to generate MUTE compared to ILP optimization. We show that MUTE can be used to train neural networks that are robust to different noisy and adversarial images while maintaining comparable accuracy on original images, yet has the same computation complexity as using one-hot target encoding.

References

- [1] Cplex. <https://www.ibm.com/analytics/cplex-optimizer>. Accessed: May 22, 2019.
- [2] Z. Akata, F. Perronnin, Z. Harchaoui, and C. Schmid. Label-embedding for image classification. *IEEE transactions on pattern analysis and machine intelligence*, 38(7):1425–1438, 2016.
- [3] Y. Amit, M. Fink, N. Srebro, and S. Ullman. Uncovering shared structures in multiclass classification. In *Proceedings of the 24th international conference on Machine learning*, pages 17–24. ACM, 2007.

- [4] Anonymous. Task-agnostic early prediction of inter-dataset similarity by using monomath autoencoders. In *Anonymous*, page 0. Anonymous, 0000.
- [5] M. M. Cisse, N. Usunier, T. Artieres, and P. Gallinari. Robust bloom filters for large multilabel classification tasks. In *Advances in Neural Information Processing Systems*, pages 1851–1859, 2013.
- [6] H. Deng, G. Stathopoulos, and C. Y. Suen. Applying error-correcting output coding to enhance convolutional neural network for target detection and pattern recognition. In *2010 20th International Conference on Pattern Recognition*, pages 4291–4294. IEEE, 2010.
- [7] T. G. Dietterich and G. Bakiri. Solving multiclass learning problems via error-correcting output codes. *Journal of artificial intelligence research*, 2:263–286, 1994.
- [8] C. M. Fiduccia and R. M. Mattheyses. A linear-time heuristic for improving network partitions. In *19th Design Automation Conference*, pages 175–181. IEEE, 1982.
- [9] A. Frome, G. S. Corrado, J. Shlens, S. Bengio, J. Dean, T. Mikolov, et al. Devise: A deep visual-semantic embedding model. In *Advances in neural information processing systems*, pages 2121–2129, 2013.
- [10] T. Gebru, J. Morgenstern, B. Vecchione, J. W. Vaughan, H. M. Wallach, H. D. III, and K. Crawford. Datasheets for datasets. *CoRR*, 2018.
- [11] I. J. Goodfellow, J. Shlens, and C. Szegedy. Explaining and harnessing adversarial examples. *arXiv preprint arXiv:1412.6572*, 2014.
- [12] K. He, X. Zhang, S. Ren, and J. Sun. Deep residual learning for image recognition. In *Proceedings of the IEEE conference on computer vision and pattern recognition*, pages 770–778, 2016.
- [13] D. Hendrycks and T. G. Dietterich. Benchmarking neural network robustness to common corruptions and surface variations. *arXiv preprint arXiv:1807.01697*, 2018.
- [14] H. Hosseini, B. Xiao, M. Jaiswal, and R. Poovendran. On the limitation of convolutional neural networks in recognizing negative images. In *2017 16th IEEE International Conference on Machine Learning and Applications (ICMLA)*, pages 352–358. IEEE, 2017.
- [15] D. J. Hsu, S. M. Kakade, J. Langford, and T. Zhang. Multi-label prediction via compressed sensing. In *Advances in neural information processing systems*, pages 772–780, 2009.
- [16] G. Huang, Z. Liu, L. van der Maaten, and K. Q. Weinberger. Densely connected convolutional networks. In *Proceedings of the IEEE Conference on Computer Vision and Pattern Recognition*, 2017.
- [17] D. Kim, S. A. Bargal, J. Zhang, and S. Sclaroff. Multi-way encoding for robustness to adversarial attacks, 2019.
- [18] A. Krizhevsky and G. Hinton. Learning multiple layers of features from tiny images. Technical report, Citeseer, 2009.
- [19] A. Krizhevsky, I. Sutskever, and G. E. Hinton. Imagenet classification with deep convolutional neural networks. In *Advances in neural information processing systems*, pages 1097–1105, 2012.
- [20] L. I. Kuncheva. Using diversity measures for generating error-correcting output codes in classifier ensembles. *Pattern Recognition Letters*, 26(1):83–90, 2005.
- [21] J. Langford and A. Beygelzimer. Sensitive error correcting output codes. In *International Conference on Computational Learning Theory*, pages 158–172. Springer, 2005.
- [22] Y. LeCun, L. Bottou, Y. Bengio, P. Haffner, et al. Gradient-based learning applied to document recognition. *Proceedings of the IEEE*, 86(11):2278–2324, 1998.
- [23] Y. Li, X. Hou, C. Koch, J. M. Rehg, and A. L. Yuille. The secrets of salient object segmentation. In *Proceedings of the IEEE Conference on Computer Vision and Pattern Recognition*, pages 280–287, 2014.
- [24] L. v. d. Maaten and G. Hinton. Visualizing data using t-sne. *Journal of machine learning research*, 9(Nov):2579–2605, 2008.
- [25] A. Madry, A. Makelov, L. Schmidt, D. Tsipras, and A. Vladu. Towards deep learning models resistant to adversarial attacks. *arXiv preprint arXiv:1706.06083*, 2017.
- [26] A. Paszke, S. Gross, S. Chintala, G. Chanan, E. Yang, Z. DeVito, Z. Lin, A. Desmaison, L. Antiga, and A. Lerer. Automatic differentiation in PyTorch. In *NIPS Autodiff Workshop*, 2017.
- [27] P. Rodríguez, M. A. Bautista, J. Gonzalez, and S. Escalera. Beyond one-hot encoding: Lower dimensional target embedding. *Image and Vision Computing*, 75:21–31, 2018.
- [28] C. Szegedy, W. Zaremba, I. Sutskever, J. Bruna, D. Erhan, I. Goodfellow, and R. Fergus. Intriguing properties of neural networks. *arXiv preprint arXiv:1312.6199*, 2013.
- [29] T. Tommasi, N. Patricia, B. Caputo, and T. Tuytelaars. A deeper look at dataset bias. In *Domain Adaptation in Computer Vision Applications*, pages 37–55. Springer, 2017.
- [30] A. Torralba, A. A. Efros, et al. Unbiased look at dataset bias. In *CVPR*, volume 1, page 7. Citeseer, 2011.
- [31] I. Tsochanaridis, T. Joachims, T. Hofmann, and Y. Altun. Large margin methods for structured and interdependent output variables. *Journal of machine learning research*, 6(Sep):1453–1484, 2005.
- [32] J. R. Ullmann. An algorithm for subgraph isomorphism. *Journal of the ACM*, 23(1):31–42, Jan. 1976.
- [33] J. Weston, S. Bengio, and N. Usunier. Large scale image annotation: learning to rank with joint word-image embeddings. *Machine learning*, 81(1):21–35, 2010.
- [34] S. Xie, R. Girshick, P. Dollár, Z. Tu, and K. He. Aggregated residual transformations for deep neural networks. In *Proceedings of the IEEE conference on computer vision and pattern recognition*, pages 1492–1500, 2017.
- [35] S. Yang, P. Luo, C. C. Loy, K. W. Shum, and X. Tang. Deep representation learning with target coding. In *Twenty-Ninth AAAI Conference on Artificial Intelligence*, 2015.
- [36] C. Zhang, S. Bengio, M. Hardt, B. Recht, and O. Vinyals. Understanding deep learning requires rethinking generalization. 2017.